

---

# Expecting The Unexpected: Towards Broad Out-Of-Distribution Detection

---

**Charles Guille-Escuret**  
ServiceNow Research, Mila,  
Université de Montréal

**Pierre-André Noël**  
ServiceNow Research

**Ioannis Mitliagkas**  
Mila, Université de Montréal,  
Canada CIFAR AI chair

**David Vazquez**  
ServiceNow Research

**Joao Monteiro**  
ServiceNow Research

## Abstract

Improving the reliability of deployed machine learning systems often involves developing methods to detect out-of-distribution (OOD) inputs. However, existing research often narrowly focuses on samples from classes that are absent from the training set, neglecting other types of plausible distribution shifts. This limitation reduces the applicability of these methods in real-world scenarios, where systems encounter a wide variety of anomalous inputs. In this study, we categorize five distinct types of distribution shifts and critically evaluate the performance of recent OOD detection methods on each of them. We publicly release our benchmark under the name BROAD (Benchmarking Resilience Over Anomaly Diversity). Our findings reveal that while these methods excel in detecting unknown classes, their performance is inconsistent when encountering other types of distribution shifts. In other words, they only reliably detect unexpected inputs that they have been specifically designed to expect. As a first step toward broad OOD detection, we learn a generative model of existing detection scores with a Gaussian mixture. By doing so, we present an ensemble approach that offers a more consistent and comprehensive solution for broad OOD detection, demonstrating superior performance compared to existing methods. Our code to download BROAD and reproduce our experiments is publicly available<sup>1</sup>

## 1 Introduction

A significant challenge in deploying modern machine learning systems in real-world scenarios is effectively handling out-of-distribution (OOD) inputs. Models are typically trained in closed-world settings with consistent data distributions, but they inevitably encounter unexpected samples when deployed in real-world environments. This can not only degrade the user experience but also potentially result in severe consequences in safety-critical applications [39, 70].

There are two primary approaches to enhancing the reliability of deployed systems: OOD robustness, which aims to improve model accuracy on shifted data distributions [17, 20], and OOD detection [82, 13], which seeks to identify potentially problematic inputs and enable appropriate actions (e.g., requesting human intervention).

When correct classification is achievable, robustness is often considered preferable since it allows the system to operate with minimal disruption. Robustness has been investigated for various types of distribution shifts [67, 26, 29]. However, attaining robustness can be challenging, and in some cases,

---

<sup>1</sup>Code to get BROAD is available at <https://github.com/ServiceNow/broad>. Code to reproduce our experiments is available as an OpenOOD [83] fork at <https://github.com/ServiceNow/broad-openood>.

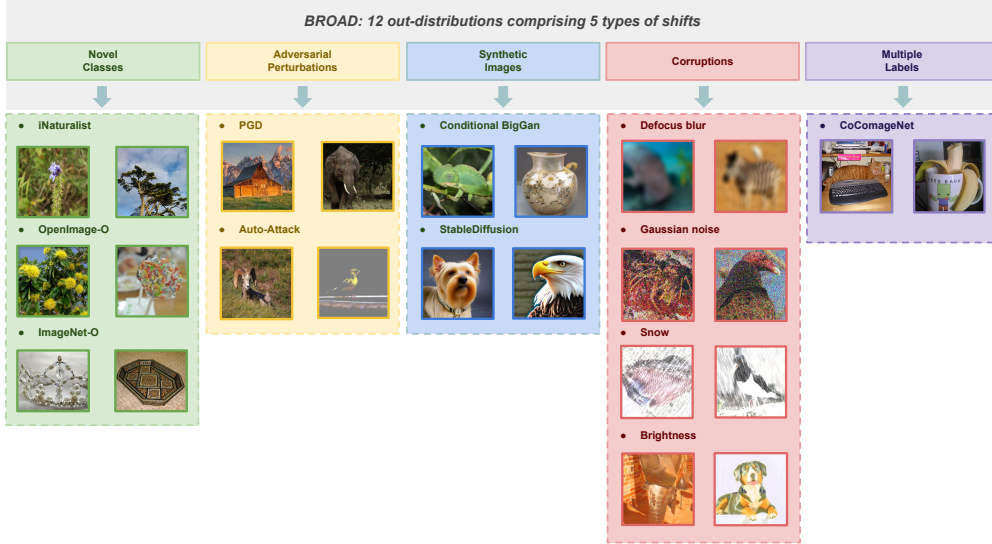


Figure 1: An overview of BROAD: illustrating the benchmarks employed for each distribution shift category, with ImageNet-1K serving as the in-distribution reference.

impossible when no known "correct" answer exists for the model to provide. OOD detection research has primarily focused on a single type of distribution shift. Despite differences in terminology and minor variations, the main settings of OOD detection in the literature—including open set recognition (OSR), anomaly detection, novelty detection, and outlier detection—primarily utilize novel classes as OOD inputs (see Yang et al. [82] for a comprehensive analysis of their differences). Previous research has explored the detection of various distribution shifts such as adversarial attacks [2, 32] and artificially generated images [35, 51, 49]. However, these studies rarely categorize them as OOD samples. While there are a few works that simultaneously detect novel labels and adversarial attacks [43, 24], the broad detection of diverse types of distribution shifts remains largely unaddressed.

This limitation significantly hinders the application of these methods in real-world scenarios. If the ultimate aim is to enhance reliability in the face of unexpected inputs that may vary in nature, then relying on homogeneous benchmarks with similar distribution shifts will likely result in methods that are overspecialized and perform unreliably on *out-of-distribution distribution shifts*. This presents a considerable limitation to existing methods, given the inherently unpredictable nature of out-of-distribution samples. Real-world systems may encounter a wide range of anomalous inputs, on which their performance are likely to degrade. Consequently, the capacity for OOD detection systems to detect an array of distribution shifts that accurately represent the variety of real-world occurrences becomes a critical imperative.

These concerns are confirmed in Figure 2, which displays the distributions of maximum softmax (MSP) [27], ViM [80], and MDS [44] scores on several shifted distributions relative to clean data

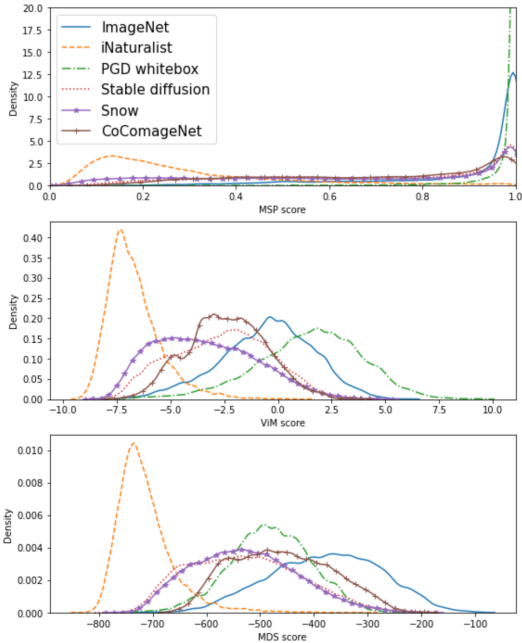


Figure 2: Figure illustrating the score distributions of MSP, ViM, and MDS across varying datasets. While all three methods successfully discriminate between ImageNet and iNaturalist, their effectiveness fluctuates across other types of distribution shifts.

(ImageNet-1k). Although all scores effectively distinguish samples from iNaturalist [33, 76], a common benchmark for detecting novel classes, their performance on other types of distribution shifts is inconsistent.

Furthermore, OOD detection methods often require tuning or even training on OOD samples [47, 44, 46], exacerbating the problem. Recent research has attempted the more challenging task of performing detection without presuming access to such samples [54, 24, 80]. Nevertheless, they may still be inherently specialized towards specific distribution shifts. For example, CSI [73] amplifies the detection score by the norm of the representations. While this improves performance on samples with novel classes (due to generally lower norm representations), it may conversely impair performance in detecting, for instance, adversarial attacks, which may exhibit abnormally high representation norms.

The scarcity of diversity in OOD detection evaluations in previous studies may be attributed to the perceived preference for OOD robustness when OOD samples share classes with the training set. Nevertheless, this preference may not always be well-founded. Firstly, previous works have indicated a potential trade-off between in-distribution accuracy and OOD robustness [75, 88], although a consensus remains elusive [85]. On the other hand, many OOD detection systems serve as post-processors that do not impact in-distribution performances. Additionally, there are practical scenarios where the detection of OOD inputs proves valuable, regardless of robustness. For instance, given the increasing prevalence of generative models [66, 62, 68], deployed systems may need to differentiate synthetic images from authentic ones, independent of performance [49, 40]. Lastly, other types of shifts exist where labels belong to the training set, but correct classification is undefined, rendering robustness unattainable (see section 2.5).

Motivated by these observations, our work concentrates on broad OOD detection, defined as the simultaneous detection of OOD samples from diverse types of distribution shifts. Our primary contributions include:

- A comprehensive benchmarking of recent OOD detection methods on BROAD, along with an analysis of their respective performance.
- The introduction of Benchmarking Resilience Over Anomaly Diversity (BROAD), an extensive OOD detection benchmark comprising datasets from five distinct types of distribution shifts relative to ImageNet: novel classes, adversarial perturbations, synthetic images, corruptions, and multi-class inputs. We also introduce CoComageNet, a subset of COCO [48]<sup>2</sup>.
- The development and evaluation of a judiciously designed generative ensemble method based on a Gaussian mixture of existing detection statistics to achieve broad detection against all types of distribution shifts, resulting in significant gains over existing methods in broad OOD detection.

Section 2 elucidates BROAD while section 3 introduces studied methods as well as our generative ensemble method based on Gaussian mixtures. In section 4, we evaluate different methods against each distribution shift. Finally, section 5 provides a synopsis of related work, while

## 2 Distribution Shift Types in BROAD

In this study, we employ ImageNet-1K [15] as our in-distribution. While previous detection studies have frequently used CIFAR [42], SVHN [60], and LSUN [86] as detection benchmarks, recent work has highlighted the limitations of these benchmarks, citing their simplicity, and has called for the exploration of detection in larger-scale settings [28]. Consequently, ImageNet has emerged as the most popular choice for in-distribution.

Our benchmark, BROAD, encompasses five distinct types of distribution shifts, each represented by one to four corresponding datasets, as summarized in Figure 1.

### 2.1 Novel Classes

The introduction of novel classes represents the most prevalent type of distribution shift in the study of OOD detection. In this scenario, the test distribution contains samples from classes not present in the training set, rendering accurate prediction unfeasible.

---

<sup>2</sup>The code and datasets are publicly available

For this particular setting, we employ three widely used benchmarks: iNaturalist [33, 76], ImageNet-O [30], and OpenImage-O [80, 41].

## 2.2 Adversarial Perturbations

Adversarial perturbations are examined using two well-established attack methods: Projected Gradient Descent (PGD)[55] and AutoAttack[12]. Each attack is generated with an  $L_\infty$  norm perturbation budget constrained to  $\epsilon = 0.05$ , with PGD employing 40 steps. In its default configuration, AutoAttack constitutes four independently computed threat models for each image; from these, we selected the one resulting in the highest confidence misclassification. A summary of the models’ predictive performance when subjected to each adversarial scheme can be found in Table 1. The relative detection difficulty of white-box versus black-box attacks remains an open question. Although white-box attacks are anticipated to introduce more pronounced perturbations to the model’s feature space, black-box attacks might push the features further away from the in-distribution samples. To elucidate this distinction and provide a more comprehensive understanding of detection performance, we generate two sets of attacks using both PGD and AutoAttack: one targeting a ResNet50 [25] and the other a Vision Transformer (ViT) [18]. Evaluation is performed on both models, thereby ensuring the inclusion of two black-box and two white-box variants for each attack.

Common practice in the field focuses on the detection of successful attacks. However, identifying failed attempts could be advantageous for security reasons. To cater to this possibility, we appraise detection methods in two distinct scenarios: the standard Distribution Shift Detection (DSD), which aims to identify any adversarial perturbation irrespective of model predictions, and Error Detection (ED), which differentiates solely between successfully perturbed samples (those initially correctly predicted by the model but subsequently misclassified following adversarial perturbation) and their corresponding original images.

Table 1: Prediction accuracy of the two evaluated models across the range of perturbation settings examined in our study.

Model	Clean Acc.	White-box		Black-box	
		PGD	AA	PGD	AA
RN50	74.2%	39.3%	28.2%	68.0%	43.3%
ViT	85.3%	0.4%	50.8%	77.1%	65.8%

## 2.3 Synthetic Images

This category of distribution shift encompasses images generated by computer algorithms. Given the rapid development of generative models, we anticipate a growing prevalence of such samples. To emulate this shift, we curated two datasets: one derived from a conditional BigGAN model [7], and another inspired by stable diffusion techniques [68].

In the case of BigGAN, we employed publicly available models<sup>3</sup> trained on ImageNet-1k and generated 25 images for each class. For our stable diffusion dataset, we utilized open-source text-conditional image generative models<sup>4</sup>. To generate images reminiscent of the ImageNet dataset, each ImageNet class was queried using the following template:

High quality image of a {class\_name}.

This procedure was repeated 25 times for each class within the ImageNet-1k label set. Given that a single ImageNet class may have multiple descriptive identifiers, we selected one at random each time.

## 2.4 Corruptions

The term *corruptions* refers to images that have undergone a range of perceptual perturbations. To simulate this type of distribution shift, we employed four distinct corruptions from ImageNet-C [26]: defocus blur, Gaussian noise, snow, and brightness. All corruptions were implemented at the maximum intensity (5 out of 5) to simulate challenging scenarios where OOD robustness is difficult, thus highlighting the importance of effective detection. Analogous to the approach taken with adversarial perturbations, we implemented two distinct evaluation scenarios: Distribution Shift

<sup>3</sup><https://github.com/lukemelas/pytorch-pretrained-gans>

<sup>4</sup><https://huggingface.co/stabilityai/stable-diffusion-2>

Table 2: Distribution shift detection AUC for Visual Transformer and ResNet-50 across different types of distribution shifts.

	Novel classes		Adv. Attacks		Synthetic		Corruptions		Multi-labels		Average	
	ViT	RN50	ViT	RN50	ViT	RN50	ViT	RN50	ViT	RN50	ViT	RN50
CADET $m_{in}$	20.91	66.79	67.12	62.4	59.82	55.65	79.67	87.15	54.24	56.88	56.35	65.77
ODIN	91.73	73.58	52.29	54.44	62.74	61.49	79.68	88.52	70.75	64.46	71.44	68.5
MAX LOGITS	95.25	73.67	59.73	59.62	66.08	57.65	83.60	90.87	71.63	62.79	75.26	68.92
LOGITS NORM	51.93	52.62	37.39	51.82	38.25	59.47	39.99	82.81	36.32	48.05	40.78	58.95
MSP	90.56	67.25	58.45	61.17	64.78	55.59	78.62	86.71	71.93	<b>67.52</b>	72.87	67.65
MDS <sub>f</sub>	53.35	63.52	67.73	55.04	54.92	56.18	31.47	76.52	63.43	36.81	54.18	57.61
MDS <sub>i</sub>	<b>97.38</b>	72.32	74.75	68.91	68.98	55.41	83.29	75.24	63.41	38.92	77.56	62.16
MDS <sub>all</sub>	89.17	72.66	<b>85.64</b>	71.49	72.45	60.89	<b>95.55</b>	89.42	26.06	30.01	73.77	64.89
REACT	95.47	79.70	60.71	61.46	66.03	54.24	83.67	89.82	71.79	63.91	75.53	69.83
GRADNORM	90.85	75.53	65.17	56.52	72.19	<b>65.57</b>	85.00	89.39	69.59	54.45	76.56	68.29
EBO	95.52	73.8	59.72	59.59	65.91	57.72	83.83	91.14	71.27	61.55	75.25	68.76
$D_\alpha$	91.27	67.95	58.62	61.44	64.95	55.65	81.57	87.43	72.49	67.15	73.78	67.92
DICE	55.7	74.45	78.29	58.76	77.84	59.43	86.67	91.38	61.23	59.97	71.95	68.8
ViM	95.76	<b>81.55</b>	56.85	62.91	61.01	53.26	79.79	87.00	68.45	49.01	72.37	66.75
ENS-V (ours)	94.97	79.42	82.67	74.85	<b>78.45</b>	60.55	92.76	91.08	73.27	53.78	<b>84.42</b>	71.93
ENS-R (ours)	95.00	80.42	80.79	<b>75.21</b>	76.56	62.38	92.17	90.56	<b>74.79</b>	60.79	83.86	<b>73.87</b>
ENS-F (ours)	95.08	79.16	79.05	69.32	75.02	59.89	91.57	<b>91.59</b>	72.55	61.41	82.65	72.27

Detection (DSD), aiming to identify corrupted images irrespective of model predictions, and Error Detection (ED), which discriminates between incorrectly classified OOD samples and correctly classified in-distribution samples, thus focusing solely on errors introduced by the distribution shift.

## 2.5 Multiple Labels

In this study, we propose CoComageNet, a new benchmark for a type of distribution shift that, to the best of our knowledge, has not been previously investigated within the context of Out-of-Distribution (OOD) detection. We specifically focus on *multiple labels* samples, which consist of at least two distinct classes from the training set occupying a substantial portion of the image.

Consider a classifier trained to differentiate dogs from cats; an image featuring both a dog and a cat side-by-side presents an ambiguous label, and classifying it as either dog or cat would be erroneous.

In safety-critical applications, this issue could result in unpredictable outcomes and requires precautionary measures, such as human intervention. For instance, a system tasked with identifying dangerous objects in images could misclassify an image featuring both a knife and a hat as safe by identifying the image as a hat.

The CoComageNet benchmark is constructed as a subset of the CoCo dataset [48], specifically, the 2017 training images. We first identify 17 CoCo classes that have equivalent counterparts in ImageNet (please refer to appendix A for a comprehensive list of the selected CoCo classes and their ImageNet equivalents). We then filter the CoCo images to include only those containing at least two different classes among the selected 17. We calculate the total area occupied by each selected class and order the filtered images based on the portion of the image occupied by the second-largest class. The top 2000 images based on this metric constitute CoComageNet. By design, each image in CoComageNet contains at least two distinct ImageNet classes occupying substantial areas.

Although CoComageNet was developed to study the detection of multiple label images, it also exhibits other less easily characterized shifts, such as differences in the properties of ImageNet and CoCo images, and the fact that CoComageNet comprises only 17 of the 1000 ImageNet classes. To isolate the effect of multiple labels, we also construct CoComageNet-mono, a similar subset of CoCo that contains only one of the selected ImageNet classes (see appendix A for details).

As shown in appendix A, detection performances for all baselines on CoComageNet-mono are near random, demonstrating that detection of CoComageNet is primarily driven by the presence of multiple labels. Finally, to reduce the impact of considering only a subset of ImageNet classes, we evaluate detection methods using in-distribution ImageNet samples from the selected classes only.

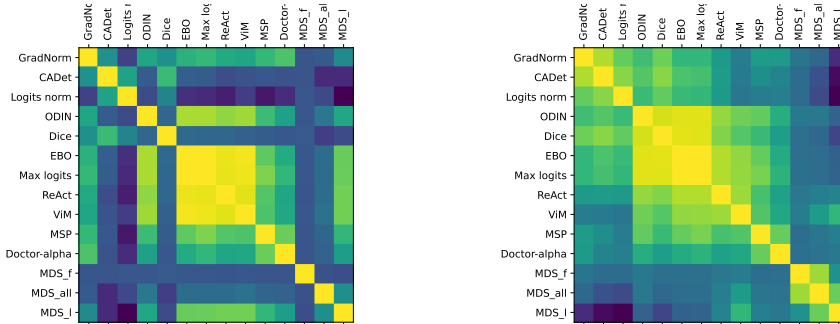


Figure 3: Covariance matrices of detection scores in-distribution for ViT (left) and ResNet-50 (right).

### 3 Detection Methods

In this study, our focus is predominantly on methods that do not require training or fine-tuning using OOD samples. This consideration closely aligns with real-world applications where OOD samples are typically not known *a priori*. Additionally, the practice of fine-tuning or training on specific types of distribution shifts heightens the risk of overfitting them.

**Evaluated Methods:** We assess a the broad OOD detection capabilities of a variety of methods including REACT [72], VIM [80], GRADNORM [34], EBO [50], DICE [71], DOCTOR [23], CADET [24], ODIN [47], and Mahalanobis Distance (MDS) [44]. Furthermore, we explore three statistics widely applied in post-hoc OOD detection: maximum softmax probabilities (MSP), maximum of logits, and logit norm.

In the case of CADET, we solely utilize the intra-similarity score  $m_{in}$  with five transformations to minimize computational demands. For DOCTOR, we employ  $D_\alpha$  in the Totally Black Box (TBB) setting, disregarding  $D_\beta$  as it is functionally equivalent to MSP in the TBB setting when rescaling the detection threshold is accounted for (resulting in identical AUC scores). ODIN typically depends on the fine-tuning of the perturbation budget  $\epsilon$  and temperature  $T$  on OOD samples. To bypass this requirement, we use default values of  $\epsilon = 0.0014$  and  $T = 1000$ . These default parameters, having been tuned on a variety of datasets and models, have demonstrated robust generalization capabilities. Nevertheless, it should be noted that the choice of these values, despite being considered reasonable, does represent a caveat, as they were initially determined by tuning OOD detection of novel classes.

In its standard form, the Mahalanobis detection method computes the layer-wise Mahalanobis distance, followed by training a logistic regressor on OOD samples to facilitate detection based on a weighted average of these distances. To eliminate the need for training on OOD samples, we consider three statistics derived from Mahalanobis distances: the Mahalanobis distance on the output of the first layer block ( $MDS_f$ ), the Mahalanobis distance on the output of the last layer ( $MDS_l$ ), and the Mahalanobis distance on the output of all layers averaged with equal weights ( $MDS_{all}$ ). For the Vision Transformer (ViT), we focus on MDS on the class token, disregarding patch tokens.

**Generative Modeling for Detection:** Consider  $\mathcal{X}$  as a data distribution with a support set denoted as  $X$ , and let  $h : X \rightarrow \mathbb{R}^d$  be a map that extracts features from a predetermined neural network. The function  $h(x)$  can be defined arbitrarily; for instance, it could be the logits that the network computes on a transformation of a sample  $x$ , or the concatenation of outputs from different layers, among other possibilities. However, generative modeling in the input space (i.e., when  $h$  is the identity function) is generally infeasible due to the exceedingly high dimensionality and intricate structure of the data.

A generative model of  $h$  is tasked with learning the distribution  $p_{x \sim \mathcal{X}}(h(x))$ , using a training set  $(x_i)_{i \leq N}$  that comprises independently sampled instances from  $\mathcal{X}$ . Given a test sample  $y$ , although it is intractable to directly infer  $p_{x \sim \mathcal{X}}(y = x)$ , it is feasible to compute  $p_{x \sim \mathcal{X}}(h(y) = h(x))$ , which can then be directly utilized as a detection score.

A significant number of detection methods devise heuristic scores on  $h$  with the aim of maximizing detection performances on specific benchmarks, while often arbitrarily discarding information that could potentially be beneficial for other distribution shifts. In contrast, generative models learn an

estimator of the likelihood of  $h(x)$  without discarding any information. Their detection performances are only constrained by the information extracted by  $h$  and, naturally, their proficiency in learning its distribution. This inherent characteristic makes generative models particularly suitable for broad Out-of-Distribution (OOD) detection. By learning the comprehensive distribution of  $h$ , these models negate the bias associated with engineering detection scores against specific distribution shifts.

**Gaussian Mixtures Ensembling:** Gaussian Mixture Models (GMMs) are a versatile tool for learning a distribution of the form:

$$x \sim \sum_i^n \pi_i \mathcal{N}(\mu_i, \Sigma_i),$$

Where  $n$  is the number of components,  $\pi$ ,  $\mu$  and  $\Sigma$  are the parameters of the GMM and are learned with the Expectation-Maximization (EM) algorithm.

The utilization of GMMs for generative modeling of neural network behaviors to facilitate detection has been previously reported [9]. Methods that are based on the Mahalanobis distance bear similarity to this approach insofar as the layer-wise Mahalanobis score can be interpreted as the likelihood of the layer output for class-dependent Gaussian distributions, which are learned from the training set.

Despite these advantages, such methods encounter the formidable challenge of learning generative models of the network’s high dimensional representation space, a task made more difficult due to the curse of dimensionality. In response to this challenge, we propose the learning of a Gaussian mixture of the scores computed by existing OOD detection methods. While this approach still relies on heuristic scores, it presents an ensemble method that is able to amalgamate their respective information, while maintaining the dimension of its underlying variables at a significantly low level. As a result, it achieves a favorable tradeoff between the generative modeling of high dimensional feature spaces and the heuristic construction of one-dimensional detection scores.

In addition to integrating their detection capabilities, this approach is adept at identifying atypical realizations of the underlying scores, even in situations where the marginal likelihood of each score is high, but their joint likelihood is low.

To make our method as general as possible, **we do not assume access to OOD samples to select which scores to use** as variables of our GMM. We present in Figure 3 the covariance matrices of the different scores on a held-out validation set of ImageNet. To minimize redundancy, we avoid picking multiple scores that are highly correlated on clean validation data. To decide between highly correlated scores, we opt for the ones with highest in-distribution error detection performance (see first two columns of Table 3). Moreover, we discard logit norm and  $MDS_f$  due to their near-random error detection performance in-distribution. Given that score correlation varies between ViTs and ResNets, as evidenced in Figure 3, we derive two distinct sets of scores. We also propose a computationally efficient alternative based on methods with minimal overhead costs:

**Ensemble-ViT** (Ens-V) = {GRADNORM, ODIN,  $MDS_{all}$ ,  $MDS_l$ , CADET, DICE, MSP, MAX LOGITS},

**Ensemble-ResNet** (Ens-R) = {GRADNORM, ODIN,  $MDS_{all}$ ,  $MDS_l$ , CADET, REACT, ViM,  $D_\alpha$ },

**Ensemble-Fast** (Ens-F) = {MSP, MAX LOGITS,  $MDS_{all}$ ,  $MDS_l$ , EBO}.

We employ a held-out validation set of 45,000 samples and discard all that are incorrectly classified to train the GMM. This is essential as misclassified samples may produce atypical values of the underlying scores despite being in-distribution, which is demonstrated by the high in-distribution error detection AUC of selected scores. Finally, we train the GMM for a number of components  $n \in \{1, 2, 5, 10, 20\}$  and select  $n = 10$  which maximizes the in-distribution error detection performances (see appendix C).

## 4 Evaluation

We assess performance using the widely accepted area under the curve (AUC) metric for two distinct pretrained models: ResNet-50 (RN50) and Vision Transformer (ViT). All evaluations are conducted on a single A100 GPU, with the inference time normalized by the cost of a forward pass (cf. App. B).

Our empirical results in the Distribution Shift Detection (DSD) setting, which aims to detect any OOD sample, are presented in Table 2. Results for the error detection setting, where the objective is

Table 3: Error detection AUC for Visual Transformer and ResNet-50 in-distribution and on two distribution shifts.

	In-distribution		Adv. Attacks		Corruptions		Average	
	ViT	RN50	ViT	RN50	ViT	RN50	ViT	RN50
CADET $m_{in}$	54.63	56.50	70.02	67.85	81.55	90.11	68.73	71.49
ODIN	75.02	75.79	56.98	62.96	90.83	95.02	74.28	77.92
MAX LOGIT	80.64	77.55	67.67	68.37	95.55	<b>96.84</b>	81.29	80.92
LOGIT NORM	36.83	50.11	34.05	55.94	33.65	84.37	34.84	63.47
MSP	<b>89.16</b>	86.31	70.29	74.04	95.75	95.93	85.07	85.43
MDS <sub>f</sub>	48.23	51.25	68.18	56.66	30.70	76.47	49.04	61.46
MDS <sub>l</sub>	74.92	55.53	82.98	72.39	96.39	75.85	84.76	67.92
MDS <sub>all</sub>	54.93	54.69	89.44	74.65	<b>99.1</b>	89.90	81.16	73.08
REACT	77.18	73.28	68.00	69.32	94.81	95.01	80.00	79.20
GRADNORM	68.01	58.07	70.92	62.49	94.00	92.73	77.64	71.10
EBO	78.35	76.02	66.63	67.63	95.01	96.61	80.00	80.09
$D_\alpha$	89.00	<b>86.50</b>	70.37	73.97	95.96	96.26	85.11	85.58
DICE	56.91	70.00	80.6	65.71	89.13	95.53	75.55	77.08
VIM	75.72	73.74	63.37	69.83	91.64	93.03	76.91	78.87
ENS-V (ours)	82.61	72.81	<b>89.52</b>	80.47	98.27	94.73	90.13	82.67
ENS-R (ours)	83.69	77.24	88.17	<b>83.79</b>	97.84	95.92	89.90	85.65
ENS-F (ours)	85.84	79.20	88.72	82.60	98.41	96.49	<b>90.99</b>	<b>86.10</b>

to detect misclassified OOD samples against correctly classified in-distribution samples, are exhibited in Table 3. The results for each distribution shift type are averaged over the corresponding benchmark. Detailed performances and model accuracy, where applicable, for each dataset are offered in Appendix D. In the error detection setting, we conduct evaluations against adversarial attacks, corruptions, and in-distribution. The latter pertains to predicting classification errors on authentic ImageNet inputs. Please note that error detection is inapplicable to novel classes and multi-labels where correct classifications are undefined, and we do not consider error detection on synthetic images as it lacks clear motivation.

**Existing methods:** A striking observation is the inconsistency of recent detection methods in the broad OOD setting. Methods that excel on adversarial attacks tend to underperform on multi-label detection, and vice versa. Each of the baselines exhibits subpar performance on at least one distribution shift, and almost all of them are Pareto-optimal. This underscores the necessity for broader OOD detection evaluations to inform the design of future methods.

We observe that while detection performances are generally superior when utilizing a ViT backbone, a finding consistent with previous studies [80], the difference is method-dependent. For instance, MDS<sub>l</sub> ranks as the best baseline on ViT (when averaged over distribution shift types), but it is the third-worst with a ResNet-50.

We further observe that many methods significantly outperform a random choice in the detection of synthetic images, regardless of the generation methods used (see Appendix D). This suggests that despite recent advancements in generative models, the task remains feasible.

Interestingly, the performance of various methods relative to others is remarkably consistent between the DSD and error detection settings, applicable to both adversarial attacks and corruptions. This consistency implies a strong correlation between efficiently detecting OOD samples and detecting errors induced by distribution shifts, suggesting that there may not be a need to compromise one objective for the other.

**Ensemble:** Our ensemble method surpasses all baselines when averaged over distribution shift types, evident in both the DSD and error detection settings, and consistent across both ViT and ResNet-50 backbones. With the exception of error detection with ResNet-50, where Doctor-alpha yields comparable results, our ensemble method consistently demonstrates significant improvements over the best-performing baselines. Specifically, in the DSD setting, ENS-V and ENS-R secure improvements of 6.86% and 4.04% for ViT and ResNet-50, respectively.

While the ensemble detection rarely surpasses the best baselines for a specific distribution shift type, it delivers more consistent performances across types, which accounts for its superior averaged AUC. This finding endorses the viability of our approach for broad OOD detection.

Despite the notable computational overhead for ENS-V and ENS-R (up to  $13.92\times$  the cost of a forward pass for ENS-V with ResNet-50, as detailed in Appendix B), the inference of ENS-F atop a

forward pass only adds a modest 19% to 25% overhead, thus striking a reasonable balance between cost and performance.

Interestingly, ENS-F trails only slightly in terms of performance in the DSD setting. In the error detection setting, ENS-F unexpectedly delivers the best results for both ViT and ResNet.

## 5 Related Work

In this work, we study the detection of out-of-distribution (OOD) samples with a broad definition of OOD, encompassing various types of distribution shifts. Our work intersects with the literature in OOD detection, adversarial detection, and synthetic image detection. We also provide a brief overview of uncertainty quantification methods that can be leveraged to detect errors induced by distribution shifts.

**Label-based OOD detection** has been extensively studied in recent years under different settings: anomaly detection [8, 64, 69], novelty detection [58, 65], open set recognition [56, 21, 6], and outlier detection [78, 31, 3]. Most existing methods can be categorized as either density-based [45, 37], reconstruction-based [16, 84], classification-based [79, 77] or distance-based [87, 74]. Methods can further be divided based on whether they require pre-processing of the input, specific training schemes, external data or can be used as post-processors on any trained model. See Yang et al. [82] for a complete survey.

**Adversarial detection** is the task of detecting adversarially perturbed inputs. Most existing methods require access to adversarial samples [2, 90, 52, 59, 53, 4, 57], with some exceptions [32, 5, 24]. Since adversarial training does not transfer well across attacks [36], adversarial detection methods that assume access to adversarial samples are also unlikely to generalize well. Unfortunately, Carlini and Wagner [10] have shown that recent detection methods can be defeated by adapting the attack’s loss function. Thus, attacks targeted against the detector typically remain undetected. However, adversarial attacks transfer remarkably well across models [11, 22], which makes deployed systems vulnerable even when the attacker does not have access to the underlying model. Detectors thus make systems more robust by requiring targeted attack designs.

**Synthetic image detection** is the detection of images that have been artificially generated. Following the rapid increase in generative models’ performances and popularity [66, 62, 68], many works have addressed the task of discriminating synthetic images from genuine ones [49]. They are generally divided between image artifact detection [49, 14, 89] and data-drive approaches [81]. Since generative models aim at learning the genuine distribution, their shortcomings only permit detection. As generative models improve, synthetic images may become indistinguishable from genuine ones.

**Uncertainty quantification (UQ)** for deep learning aims to improve the estimation of neural network confidences. Neural networks tend to be overconfident even on samples far from the training distribution [61]. By better estimating the confidence in the network’s predictions, uncertainty quantification can help detect errors induced by distribution shifts. See Abdar et al. [1], Kabir et al. [38], Ning and You [63] for overviews of UQ in deep learning.

**Detection of multiple types of distribution shifts** has been addressed by relatively few prior works. The closest work in the literature is probably Guille-Escuret et al. [24] and Lee et al. [44] which aims at simultaneously detecting novel classes and adversarial samples. In comparison, this work evaluates detection methods on five different types of distribution shifts. To the best of our knowledge, it is the first time that such broad OOD detection is studied in the literature.

## 6 Conclusion

We have evaluated recent OOD detection methods on BROAD, a diversified benchmark spanning 5 different distribution shift types, and found their performances unreliable. Due to the literature focusing on specific distribution shifts, existing methods often fail to detect samples of certain out-of-distribution shifts.

To design systems capable of detecting a broad range of unexpected inputs, we have proposed an ensemble method based on Gaussian mixtures to combine the respective strengths of existing detection scores, and found it to obtain significant gains compared to previous works, even when limiting overhead computations to 25%.

We encourage future work to consider more varied types of OOD samples for their detection evaluations, so that future methods will not see their success limited to unexpected inputs that are expected.

## References

- [1] M. Abdar, F. Pourpanah, S. Hussain, D. Rezazadegan, L. Liu, M. Ghavamzadeh, P. Fieguth, X. Cao, A. Khosravi, U. R. Acharya, V. Makarenkov, and S. Nahavandi. A review of uncertainty quantification in deep learning: Techniques, applications and challenges. *Information Fusion*, 76:243–297, 2021. ISSN 1566-2535. doi: <https://doi.org/10.1016/j.inffus.2021.05.008>. URL <https://www.sciencedirect.com/science/article/pii/S1566253521001081>.
- [2] A. Abusnaina, Y. Wu, S. Arora, Y. Wang, F. Wang, H. Yang, and D. Mohaisen. Adversarial example detection using latent neighborhood graph. In *International Conference on Computer Vision*, 2021.
- [3] C. C. Aggarwal and P. S. Yu. Outlier detection for high dimensional data. In *Proceedings of the 2001 ACM SIGMOD International Conference on Management of Data*, SIGMOD '01, page 37–46, New York, NY, USA, 2001. Association for Computing Machinery. ISBN 1581133324. doi: 10.1145/375663.375668. URL <https://doi.org/10.1145/375663.375668>.
- [4] Z. Akhtar, J. Monteiro, and T. H. Falk. Adversarial examples detection using no-reference image quality features. In *2018 international Carnahan conference on security technology (ICCST)*, pages 1–5. IEEE, 2018.
- [5] A. N. Bhagoji, D. Cullina, and P. Mittal. Dimensionality reduction as a defense against evasion attacks on machine learning classifiers. *ArXiv*, abs/1704.02654, 2017.
- [6] T. Boulton, S. Cruz, A. Dhamija, M. Günther, J. Henrydoss, and W. Scheirer. Learning and the unknown: Surveying steps toward open world recognition. *Proceedings of the AAAI Conference on Artificial Intelligence*, 33:9801–9807, 07 2019. doi: 10.1609/aaai.v33i01.33019801.
- [7] A. Brock, J. Donahue, and K. Simonyan. Large scale GAN training for high fidelity natural image synthesis. In *7th International Conference on Learning Representations, ICLR 2019, New Orleans, LA, USA, May 6-9, 2019*. OpenReview.net, 2019. URL <https://openreview.net/forum?id=B1xsqj09Fm>.
- [8] S. Bulusu, B. Kailkhura, B. Li, P. K. Varshney, and D. X. Song. Anomalous example detection in deep learning: A survey. *IEEE Access*, 8:132330–132347, 2020.
- [9] A. Cao, Y. Luo, and D. Klabjan. Open-set recognition with gaussian mixture variational autoencoders. *CoRR*, abs/2006.02003, 2020. URL <https://arxiv.org/abs/2006.02003>.
- [10] N. Carlini and D. A. Wagner. Adversarial examples are not easily detected: Bypassing ten detection methods. *CoRR*, abs/1705.07263, 2017. URL <http://arxiv.org/abs/1705.07263>.
- [11] A. Chaubey, N. Agrawal, K. Barnwal, K. K. Guliani, and P. Mehta. Universal adversarial perturbations: A survey. *CoRR*, abs/2005.08087, 2020. URL <https://arxiv.org/abs/2005.08087>.
- [12] F. Croce and M. Hein. Reliable evaluation of adversarial robustness with an ensemble of diverse parameter-free attacks. In *Proceedings of the 37th International Conference on Machine Learning, ICML'20*. JMLR.org, 2020.
- [13] P. Cui and J. Wang. Out-of-distribution (ood) detection based on deep learning: A review. *Electronics*, 11(21), 2022. ISSN 2079-9292. doi: 10.3390/electronics11213500. URL <https://www.mdpi.com/2079-9292/11/21/3500>.
- [14] H. Dang\*, F. Liu\*, J. Stehouwer\*, X. Liu, and A. Jain. On the detection of digital face manipulation. In *In Proceeding of IEEE Computer Vision and Pattern Recognition*, Seattle, WA, June 2020.
- [15] J. Deng, W. Dong, R. Socher, L.-J. Li, K. Li, and L. Fei-Fei. Imagenet: A large-scale hierarchical image database. In *2009 IEEE Conference on Computer Vision and Pattern Recognition*, pages 248–255, 2009. doi: 10.1109/CVPR.2009.5206848.
- [16] T. Denouden, R. Salay, K. Czarnecki, V. Abdelzad, B. Phan, and S. Vernekar. Improving reconstruction autoencoder out-of-distribution detection with mahalanobis distance. *CoRR*, abs/1812.02765, 2018. URL <http://arxiv.org/abs/1812.02765>.
- [17] S. F. Dodge and L. J. Karam. A study and comparison of human and deep learning recognition performance under visual distortions. *CoRR*, abs/1705.02498, 2017. URL <http://arxiv.org/abs/1705.02498>.

- [18] A. Dosovitskiy, L. Beyer, A. Kolesnikov, D. Weissenborn, X. Zhai, T. Unterthiner, M. Dehghani, M. Minderer, G. Heigold, S. Gelly, J. Uszkoreit, and N. Houlsby. An image is worth 16x16 words: Transformers for image recognition at scale, 2020. URL <https://arxiv.org/abs/2010.11929>.
- [19] C. Fellbaum. *WordNet: An Electronic Lexical Database*. MIT Press, Cambridge, MA, 1998.
- [20] R. Geirhos, J. Jacobsen, C. Michaelis, R. S. Zemel, W. Brendel, M. Bethge, and F. A. Wichmann. Shortcut learning in deep neural networks. *CoRR*, abs/2004.07780, 2020. URL <https://arxiv.org/abs/2004.07780>.
- [21] C. Geng, S.-J. Huang, and S. Chen. Recent advances in open set recognition: A survey. *IEEE transactions on pattern analysis and machine intelligence*, 43(10):3614–3631, October 2021. ISSN 0162-8828. doi: 10.1109/tpami.2020.2981604. URL <https://doi.org/10.1109/TPAMI.2020.2981604>.
- [22] I. J. Goodfellow, J. Shlens, and C. Szegedy. Explaining and harnessing adversarial examples. In Y. Bengio and Y. LeCun, editors, *3rd International Conference on Learning Representations, ICLR 2015, San Diego, CA, USA, May 7-9, 2015, Conference Track Proceedings*, 2015. URL <http://arxiv.org/abs/1412.6572>.
- [23] F. Granese, M. Romanelli, D. Gorla, C. Palamidessi, and P. Piantanida. DOCTOR: A simple method for detecting misclassification errors. In A. Beygelzimer, Y. Dauphin, P. Liang, and J. W. Vaughan, editors, *Advances in Neural Information Processing Systems*, 2021. URL <https://openreview.net/forum?id=FHQBDiMwvK>.
- [24] C. Guille-Escuret, P. Rodriguez, D. Vazquez, I. Mitliagkas, and J. Monteiro. Cadet: Fully self-supervised anomaly detection with contrastive learning, 2022. URL <https://arxiv.org/abs/2210.01742>.
- [25] K. He, X. Zhang, S. Ren, and J. Sun. Deep residual learning for image recognition. *arXiv preprint arXiv:1512.03385*, 2015.
- [26] D. Hendrycks and T. G. Dietterich. Benchmarking neural network robustness to common corruptions and perturbations. *CoRR*, abs/1903.12261, 2019. URL <http://arxiv.org/abs/1903.12261>.
- [27] D. Hendrycks and K. Gimpel. A baseline for detecting misclassified and out-of-distribution examples in neural networks. *arXiv preprint arXiv:1610.02136*, 2016.
- [28] D. Hendrycks, S. Basart, M. Mazeika, A. Zou, J. Kwon, M. Mostajabi, J. Steinhardt, and D. Song. Scaling out-of-distribution detection for real-world settings. *arXiv preprint arXiv:1911.11132*, 2019.
- [29] D. Hendrycks, S. Basart, N. Mu, S. Kadavath, F. Wang, E. Dorundo, R. Desai, T. Zhu, S. Parajuli, M. Guo, D. Song, J. Steinhardt, and J. Gilmer. The many faces of robustness: A critical analysis of out-of-distribution generalization. *CoRR*, abs/2006.16241, 2020. URL <https://arxiv.org/abs/2006.16241>.
- [30] D. Hendrycks, K. Zhao, S. Basart, J. Steinhardt, and D. Song. Natural adversarial examples. *arXiv preprint arXiv:1907.07174*, 2021.
- [31] V. Hodge and J. Austin. A survey of outlier detection methodologies. *Artificial Intelligence Review*, 22:85–126, 10 2004. doi: 10.1023/B:AIRE.0000045502.10941.a9.
- [32] S. Hu, T. Yu, C. Guo, W.-L. Chao, and K. Q. Weinberger. A new defense against adversarial images: Turning a weakness into a strength. In *Advances in Neural Information Processing Systems*, 2019.
- [33] R. Huang and Y. Li. Mos: Towards scaling out-of-distribution detection for large semantic space. *arXiv preprint arXiv:2105.01879*, 2021.
- [34] R. Huang, A. Geng, and Y. Li. On the importance of gradients for detecting distributional shifts in the wild. *CoRR*, abs/2110.00218, 2021. URL <https://arxiv.org/abs/2110.00218>.
- [35] N. Hulzebosch, S. Ibrahimi, and M. Worring. Detecting cnn-generated facial images in real-world scenarios. *CoRR*, abs/2005.05632, 2020. URL <https://arxiv.org/abs/2005.05632>.
- [36] A. Ibrahim, C. Guille-Escuret, I. Mitliagkas, I. Rish, D. Krueger, and P. Bashivan. Towards out-of-distribution adversarial robustness, 2022. URL <https://arxiv.org/abs/2210.03150>.

- [37] D. Jiang, S. Sun, and Y. Yu. Revisiting flow generative models for out-of-distribution detection. In *International Conference on Learning Representations*, 2022. URL <https://openreview.net/forum?id=6y2KBh-0Fd9>.
- [38] H. M. D. Kabir, A. Khosravi, M. A. Hosen, and S. Nahavandi. Neural network-based uncertainty quantification: A survey of methodologies and applications. *IEEE Access*, 6:36218–36234, 2018. doi: 10.1109/ACCESS.2018.2836917.
- [39] B. Kitt, A. Geiger, and H. Lategahn. Visual odometry based on stereo image sequences with ransac-based outlier rejection scheme. In *2010 IEEE Intelligent Vehicles Symposium*, pages 486–492, 2010. doi: 10.1109/IVS.2010.5548123.
- [40] P. Korshunov and S. Marcel. Deepfakes: a new threat to face recognition? assessment and detection. *CoRR*, abs/1812.08685, 2018. URL <http://arxiv.org/abs/1812.08685>.
- [41] I. Krasin, T. Duerig, N. Alldrin, A. Veit, S. Abu-El-Haija, S. Belongie, D. Cai, Z. Feng, V. Ferrari, and V. Gomes. Openimages: A public dataset for large-scale multi-label and multi-class image classification., 01 2016.
- [42] A. Krizhevsky. Learning multiple layers of features from tiny images. Technical report, University of Toronto, 2009.
- [43] K. Lee, K. Lee, H. Lee, and J. Shin. A simple unified framework for detecting out-of-distribution samples and adversarial attacks. In *Proceedings of the 32nd International Conference on Neural Information Processing Systems, NIPS’18*, page 7167–7177, Red Hook, NY, USA, 2018. Curran Associates Inc.
- [44] K. Lee, K. Lee, H. Lee, and J. Shin. A simple unified framework for detecting out-of-distribution samples and adversarial attacks. In *Advances in Neural Information Processing Systems*, 2018.
- [45] C.-L. Li, K. Sohn, J. Yoon, and T. Pfister. Cutpaste: Self-supervised learning for anomaly detection and localization. In *2021 IEEE/CVF Conference on Computer Vision and Pattern Recognition (CVPR)*, pages 9659–9669, 2021. doi: 10.1109/CVPR46437.2021.00954.
- [46] S. Liang, Y. Li, and R. Srikant. Principled detection of out-of-distribution examples in neural networks. *CoRR*, abs/1706.02690, 2017. URL <http://arxiv.org/abs/1706.02690>.
- [47] S. Liang, Y. Li, and R. Srikant. Enhancing the reliability of out-of-distribution image detection in neural networks. *arXiv preprint arXiv:1706.02690*, 2017.
- [48] T. Lin, M. Maire, S. J. Belongie, L. D. Bourdev, R. B. Girshick, J. Hays, P. Perona, D. Ramanan, P. Dollár, and C. L. Zitnick. Microsoft COCO: common objects in context. *CoRR*, abs/1405.0312, 2014. URL <http://arxiv.org/abs/1405.0312>.
- [49] B. Liu, F. Yang, X. Bi, B. Xiao, W. Li, and X. Gao. Detecting generated images by real images. In *Computer Vision – ECCV 2022: 17th European Conference, Tel Aviv, Israel, October 23–27, 2022, Proceedings, Part XIV*, page 95–110, Berlin, Heidelberg, 2022. Springer-Verlag. ISBN 978-3-031-19780-2. doi: 10.1007/978-3-031-19781-9\_6. URL [https://doi.org/10.1007/978-3-031-19781-9\\_6](https://doi.org/10.1007/978-3-031-19781-9_6).
- [50] W. Liu, X. Wang, J. Owens, and Y. Li. Energy-based out-of-distribution detection. In *Advances in Neural Information Processing Systems*, 2020.
- [51] Z. Liu, X. Qi, J. Jia, and P. H. S. Torr. Global texture enhancement for fake face detection in the wild. *CoRR*, abs/2002.00133, 2020. URL <https://arxiv.org/abs/2002.00133>.
- [52] J. Lust and A. P. Condurache. Gran: an efficient gradient-norm based detector for adversarial and misclassified examples. *arXiv preprint arXiv:2004.09179*, 2020.
- [53] X. Ma, B. Li, Y. Wang, S. M. Erfani, S. Wijewickrema, G. Schoenebeck, D. Song, M. E. Houle, and J. Bailey. Characterizing adversarial subspaces using local intrinsic dimensionality. *arXiv preprint arXiv:1801.02613*, 2018.
- [54] D. Macêdo and T. B. Ludermir. Improving entropic out-of-distribution detection using isometric distances and the minimum distance score. *CoRR*, abs/2105.14399, 2021. URL <https://arxiv.org/abs/2105.14399>.
- [55] A. Madry, A. Makelov, L. Schmidt, D. Tsipras, and A. Vladu. Towards deep learning models resistant to adversarial attacks. *arXiv preprint arXiv:1706.06083*, 2017.

- [56] A. Mahdavi and M. Carvalho. A survey on open set recognition. In *2021 IEEE Fourth International Conference on Artificial Intelligence and Knowledge Engineering (AIKE)*, pages 37–44, Los Alamitos, CA, USA, dec 2021. IEEE Computer Society. doi: 10.1109/AIKE52691.2021.00013. URL <https://doi.ieeecomputersociety.org/10.1109/AIKE52691.2021.00013>.
- [57] J. H. Metzen, T. Genewein, V. Fischer, and B. Bischoff. On detecting adversarial perturbations. *arXiv preprint arXiv:1702.04267*, 2017.
- [58] D. Miljković. Review of novelty detection methods. In *MIPRO*, pages 593–598, 05 2010. ISBN 978-1-4244-7763-0.
- [59] J. Monteiro, I. Albuquerque, Z. Akhtar, and T. H. Falk. Generalizable adversarial examples detection based on bi-model decision mismatch. In *International Conference on Systems, Man and Cybernetics (SMC)*, 2019.
- [60] Y. Netzer, T. Wang, A. Coates, A. Bissacco, B. Wu, and A. Y. Ng. Reading digits in natural images with unsupervised feature learning. In *NIPS Workshop on Deep Learning and Unsupervised Feature Learning 2011*, 2011.
- [61] A. Nguyen, J. Yosinski, and J. Clune. Deep neural networks are easily fooled: High confidence predictions for unrecognizable images. In *2015 IEEE Conference on Computer Vision and Pattern Recognition (CVPR)*, pages 427–436, 2015. doi: 10.1109/CVPR.2015.7298640.
- [62] A. Q. Nichol, P. Dhariwal, A. Ramesh, P. Shyam, P. Mishkin, B. McGrew, I. Sutskever, and M. Chen. GLIDE: towards photorealistic image generation and editing with text-guided diffusion models. In K. Chaudhuri, S. Jegelka, L. Song, C. Szepesvári, G. Niu, and S. Sabato, editors, *International Conference on Machine Learning, ICML 2022, 17-23 July 2022, Baltimore, Maryland, USA*, volume 162 of *Proceedings of Machine Learning Research*, pages 16784–16804. PMLR, 2022. URL <https://proceedings.mlr.press/v162/nichol22a.html>.
- [63] C. Ning and F. You. Optimization under uncertainty in the era of big data and deep learning: When machine learning meets mathematical programming. *Computers and Chemical Engineering*, 125:434–448, 2019. ISSN 0098-1354. doi: <https://doi.org/10.1016/j.compchemeng.2019.03.034>. URL <https://www.sciencedirect.com/science/article/pii/S0098135419300687>.
- [64] G. Pang, C. Shen, L. Cao, and A. V. D. Hengel. Deep learning for anomaly detection: A review. *ACM Comput. Surv.*, 54(2), mar 2021. ISSN 0360-0300. doi: 10.1145/3439950. URL <https://doi.org/10.1145/3439950>.
- [65] M. A. Pimentel, D. A. Clifton, L. Clifton, and L. Tarassenko. A review of novelty detection. *Signal Processing*, 99:215–249, 2014. ISSN 0165-1684. doi: <https://doi.org/10.1016/j.sigpro.2013.12.026>. URL <https://www.sciencedirect.com/science/article/pii/S016516841300515X>.
- [66] A. Ramesh, P. Dhariwal, A. Nichol, C. Chu, and M. Chen. Hierarchical text-conditional image generation with CLIP latents. *CoRR*, abs/2204.06125, 2022. doi: 10.48550/arXiv.2204.06125. URL <https://doi.org/10.48550/arXiv.2204.06125>.
- [67] B. Recht, R. Roelofs, L. Schmidt, and V. Shankar. Do imagenet classifiers generalize to imagenet? *CoRR*, abs/1902.10811, 2019. URL <http://arxiv.org/abs/1902.10811>.
- [68] R. Rombach, A. Blattmann, D. Lorenz, P. Esser, and B. Ommer. High-resolution image synthesis with latent diffusion models. In *Proceedings of the IEEE Conference on Computer Vision and Pattern Recognition (CVPR)*, 2022. URL <https://github.com/CompVis/latent-diffusionhttps://arxiv.org/abs/2112.10752>.
- [69] L. Ruff, J. Kauffmann, R. Vandermeulen, G. Montavon, W. Samek, M. Kloft, T. Dietterich, and K.-R. Müller. A unifying review of deep and shallow anomaly detection. *Proceedings of the IEEE*, PP:1–40, 02 2021. doi: 10.1109/JPROC.2021.3052449.
- [70] T. Schlegl, P. Seeböck, S. M. Waldstein, U. Schmidt-Erfurth, and G. Langs. Unsupervised anomaly detection with generative adversarial networks to guide marker discovery. In *International conference on information processing in medical imaging*, 2017.
- [71] Y. Sun and Y. Li. Dice: Leveraging sparsification for out-of-distribution detection, 2021. URL <https://arxiv.org/abs/2111.09805>.

- [72] Y. Sun, C. Guo, and Y. Li. React: Out-of-distribution detection with rectified activations. *arXiv preprint arXiv:2111.12797*, 2021.
- [73] J. Tack, S. Mo, J. Jeong, and J. Shin. Csi: Novelty detection via contrastive learning on distributionally shifted instances. In *Advances in Neural Information Processing Systems*, 2020.
- [74] E. Techapanurak, M. Suganuma, and T. Okatani. Hyperparameter-free out-of-distribution detection using cosine similarity. In *Proceedings of the Asian Conference on Computer Vision (ACCV)*, November 2020.
- [75] D. Tsipras, S. Santurkar, L. Engstrom, A. Turner, and A. Madry. Robustness may be at odds with accuracy. In *7th International Conference on Learning Representations, ICLR 2019, New Orleans, LA, USA, May 6-9, 2019*. OpenReview.net, 2019. URL <https://openreview.net/forum?id=SyxAb30cY7>.
- [76] G. Van Horn, O. Mac Aodha, Y. Song, Y. Cui, C. Sun, A. Shepard, H. Adam, P. Perona, and S. Belongie. The inaturalist species classification and detection dataset, 2017. URL <https://arxiv.org/abs/1707.06642>.
- [77] A. Vyas, N. Jammalamadaka, X. Zhu, D. Das, B. Kaul, and T. L. Willke. Out-of-distribution detection using an ensemble of self supervised leave-out classifiers. In V. Ferrari, M. Hebert, C. Sminchisescu, and Y. Weiss, editors, *Computer Vision – ECCV 2018*, pages 560–574, Cham, 2018. Springer International Publishing. ISBN 978-3-030-01237-3.
- [78] H. Wang, M. J. Bah, and M. Hammad. Progress in outlier detection techniques: A survey. *IEEE Access*, 7:107964–108000, 2019. doi: 10.1109/ACCESS.2019.2932769.
- [79] H. Wang, W. Liu, A. Bocchieri, and Y. Li. Can multi-label classification networks know what they don’t know? *CoRR*, abs/2109.14162, 2021. URL <https://arxiv.org/abs/2109.14162>.
- [80] H. Wang, Z. Li, L. Feng, and W. Zhang. Vim: Out-of-distribution with virtual-logit matching. In *Conference on Computer Vision and Pattern Recognition*, 2022.
- [81] S. Wang, O. Wang, R. Zhang, A. Owens, and A. A. Efros. Cnn-generated images are surprisingly easy to spot... for now. *CoRR*, abs/1912.11035, 2019. URL <http://arxiv.org/abs/1912.11035>.
- [82] J. Yang, K. Zhou, Y. Li, and Z. Liu. Generalized out-of-distribution detection: A survey. *CoRR*, abs/2110.11334, 2021. URL <https://arxiv.org/abs/2110.11334>.
- [83] J. Yang, P. Wang, D. Zou, Z. Zhou, K. Ding, W. Peng, H. Wang, G. Chen, B. Li, Y. Sun, X. Du, K. Zhou, W. Zhang, D. Hendrycks, Y. Li, and Z. Liu. Openood: Benchmarking generalized out-of-distribution detection. *OpenReview*, 2022.
- [84] Y. Yang, R. Gao, and Q. Xu. Out-of-distribution detection with semantic mismatch under masking. In S. Avidan, G. Brostow, M. Cissé, G. M. Farinella, and T. Hassner, editors, *Computer Vision – ECCV 2022*, pages 373–390, Cham, 2022. Springer Nature Switzerland. ISBN 978-3-031-20053-3.
- [85] Y.-Y. Yang, C. Rashtchian, H. Zhang, R. R. Salakhutdinov, and K. Chaudhuri. A closer look at accuracy vs. robustness. In H. Larochelle, M. Ranzato, R. Hadsell, M. Balcan, and H. Lin, editors, *Advances in Neural Information Processing Systems*, volume 33, pages 8588–8601. Curran Associates, Inc., 2020. URL <https://proceedings.neurips.cc/paper/2020/file/61d77652c97ef636343742fc3dcf3ba9-Paper.pdf>.
- [86] F. Yu, A. Seff, Y. Zhang, S. Song, T. Funkhouser, and J. Xiao. Lsun: Construction of a large-scale image dataset using deep learning with humans in the loop. *arXiv preprint arXiv:1506.03365*, 2015.
- [87] A. Zaemzadeh, N. Bisagno, Z. Sambugaro, N. Conci, N. Rahnavard, and M. Shah. Out-of-distribution detection using union of 1-dimensional subspaces. In *2021 IEEE/CVF Conference on Computer Vision and Pattern Recognition (CVPR)*, pages 9447–9456, 2021. doi: 10.1109/CVPR46437.2021.00933.
- [88] H. Zhang, Y. Yu, J. Jiao, E. P. Xing, L. E. Ghaoui, and M. I. Jordan. Theoretically principled trade-off between robustness and accuracy. *CoRR*, abs/1901.08573, 2019. URL <http://arxiv.org/abs/1901.08573>.

- [89] H. Zhao, T. Wei, W. Zhou, W. Zhang, D. Chen, and N. Yu. Multi-attentional deepfake detection. In *2021 IEEE/CVF Conference on Computer Vision and Pattern Recognition (CVPR)*, pages 2185–2194, Los Alamitos, CA, USA, jun 2021. IEEE Computer Society. doi: 10.1109/CVPR46437.2021.00222. URL <https://doi.ieeecomputersociety.org/10.1109/CVPR46437.2021.00222>.
- [90] F. Zuo and Q. Zeng. Exploiting the sensitivity of l2 adversarial examples to erase-and-restore. In *Asia Conference on Computer and Communications Security*, 2021.

## A CoComageNet

Table 4: CoCo and ImageNet classes used for CoComageNet and CoComageNet-mono.

CoCo		ImageNet	
ID	Name	ID	Name
24	Zebra	n02391049	Zebra
27	Backpack	n02769748	Backpack, back pack, knapsack, packsack, rucksack, haversack
28	Umbrella	n04507155	Umbrella
35	Skis	n04228054	Ski
38	Kite	n01608432	Kite
47	Cup	n07930864	Cup
52	Banana	n07753592	Banana
55	Orange	n07747607	Orange
56	Broccoli	n07714990	Broccoli
59	Pizza	n07873807	Pizza, pizza pie
73	Laptop	n03642806	Laptop, laptop computer
74	Mouse	n03793489	Mouse, computer mouse
75	Remote	n04074963	Remote control, remote
78	Microwave	n03761084	Microwave, microwave oven
80	Toaster	n04442312	Toaster
82	Refrigerator	n04070727	Refrigerator, icebox
86	Vase	n04522168	Vase

We here provide additional information related to the CoComageNet and CoComageNet-mono datasets, together referred to as CoComageNet.

Table 4 lists the classes used for CoComageNet with their corresponding IDs and names for both CoCo and ImageNet. These classes were automatically selected by finding matches between CoCo names and ImageNet IDs understood as WordNet synsets [19]. Only exact matches were considered; hyponyms and hypernyms were excluded. While one could argue for more classes to be added to this list, we believe that those present on this list are “safe”.

CoComageNet, introduced in section 2.5, aims to induce a distribution shift due to the presence of multiple classes. However, it is also affected by the distributional variations between ImageNet and CoCo, such as different angles, distances, brightness, etc.

To alleviate this issue, we introduce the sister dataset CoComageNet-mono by selecting 2000 different images from the same CoCo 2017 training dataset. Disregarding any “Person” CoCo label, we only keep the images whose labels belong to a single CoCo class, and only if that class is one of the 17 listed in table 4. For example, the photograph of a person holding several bananas satisfies these conditions (disregarding the person, the labels are all in the same “banana” class) while one with a cat next to a banana does not (even though “cat” is not listed in table 4, it is a CoCo class). For classes with less than 157 images left, we add all these images to CoComageNet-mono. For the other classes, we sort the images of each class according to the

Table 5: Detection AUC of ResNet-50 and ViT for different detection scores against CoComageNet and CoComageNet-mono

	CoComageNet		CoComageNet-mono	
	ViT	RN-50	ViT	RN-50
CADet $m_{in}$	54.24	56.88	52.24	50.8
ODIN	70.75	64.46	55.27	53.72
Max logits	71.63	62.79	56.15	53.32
Logit norm	36.32	48.05	51.03	55.26
MSP	71.93	67.52	53.16	53.32
MDS <sub>f</sub>	63.43	36.81	61.38	48.45
MDS <sub>l</sub>	63.41	38.92	58.32	50.97
MDS <sub>all</sub>	26.06	30.01	46.66	47.06
ReAct	71.79	63.91	57.81	58.73
GradNorm	69.59	54.45	56.34	53.43
EBO	71.27	61.55	56.65	53.31
$D_\alpha$	72.49	67.15	53.41	53.08
Dice	61.23	59.97	57.35	53.00
ViM	68.45	49.01	57.06	54.54
Ens-V (us)	73.22	61.29	59.21	59.06
Ens-R (us)	74.79	61.01	60.29	56.75
Ens-F (us)	72.65	61.42	58.92	58.34

Table 6: Normalized inference time.

	ViT	RN-50
Forward	1.00	1.00
Cadet $m_{in}$	5.04	5.15
Odin	3.22	2.94
max logit	1.01	1.00
logit norm	1.01	1.00
MSP	1.01	1.00
MDS <sub>f</sub>	1.23	1.17
MDS <sub>l</sub>	1.23	1.17
MDS <sub>all</sub>	1.23	1.17
ReAct	1.11	1.06
GradNorm	2.28	3.86
EBO	1.01	1.03
$D_{\alpha}$	1.01	1.06
Dice	1.03	1.09
ViM	3.64	2.03
Ens-V (us)	11.53	13.92
Ens-R (us)	10.25	10.92
Ens-F (us)	1.25	1.19

proportion of the image taken by that class, and add to CoComageNet-mono the top 157 by that metric (top 158 for the two most populated classes), for a total of 2000 images.

Table 5 shows the detection performances of all baselines and our method against CoComageNet and CoComageNet-mono. Detection performances on CoComageNet-mono are generally close to 50% (corresponding to random guess) which shows that the distribution shift between ImageNet and CoCo has limited influence on the detection scores of our baselines. In comparison, detection scores are generally significantly further from 50% on CoComageNet, showing it is indeed the presence of multiple classes that drives detection in the case of CoComageNet.

## B Computation time

Table 6 presents the computation time of each method, normalized by the cost of a forward pass. Note that when normal inference is needed to compute the score, its computation time is included in the inference time. Therefore, running Ens-S on top of classification only has an additional overhead of 25% for ViT and 19% for ResNet.

## C Number of components

We present in Table 7 and Table 8 the in-distribution error detection AUCs that were used to pick the number of components  $n$  of the Gaussian mixture. We observe that the number of components has a low impact on performances, and that in-distribution error detection AUC has a clear correlation with broad OOD detection performances, making it an adequate metric to determine the number of components.

Table 7: In-distribution error detection AUC and OOD detection AUC averaged over distribution shift types, for a ResNet-50 using Ensemble-ResNet and using  $n$  Gaussian components.

$n$	In-dist error detection	Avg OOD detection
1	74.99	71.85
2	76.02	73.08
5	77.13	<b>73.51</b>
10	<b>77.24</b>	73.46
20	75.16	71.44

Table 8: In-distribution error detection AUC and OOD detection AUC averaged over distribution shift types, for a ViT using Ensemble-ViT and using n Gaussian components.

n	In-dist error detection	Avg OOD detection
1	82.41	82.91
2	82.34	83.20
5	82.59	83.61
10	<b>82.61</b>	<b>83.66</b>
20	82.19	81.80

## D Complete results

In this section, we provide in Table 9 to Table 15 the detection AUC of all methods against each dataset separately, both in the DSD and the error detection setting.

Table 9: AUC for OOD detection in DSD setting for ResNet on novel classes datasets.

	iNat	OI-O	INet-O
CADet $m_{in}$	88.08	74.41	37.88
ODIN	91.19	88.26	41.28
Max logits	91.17	89.14	40.69
Logits norm	55.98	66.19	35.68
MSP	88.34	84.85	28.55
MDS <sub>f</sub>	63.14	61.70	65.71
MDS <sub>l</sub>	63.18	69.32	<b>84.45</b>
MDS <sub>all</sub>	61.42	72.81	83.74
ReAct	<b>96.39</b>	<b>90.33</b>	52.37
GradNorm	93.90	84.79	47.9
EBO	90.63	89.03	41.75
$D_\alpha$	89.43	85.84	28.57
Dice	92.50	88.25	42.61
ViM	88.15	88.05	68.45
Ens-V (us)	85.50	81.96	70.81
Ens-R (us)	89.40	86.11	65.74
Ens-F (us)	88.06	86.64	62.79

Table 10: AUC for OOD detection in DSD setting for ResNet on synthetic datasets.

	Biggan	diffusion
Accuracy %	88.61	47.38
CADet $m_{in}$	63.18	48.12
ODIN	44.46	78.51
Max logits	42.14	73.15
Logits norm	59.73	59.21
MSP	41.37	69.81
MDS <sub>f</sub>	38.25	74.11
MDS <sub>l</sub>	38.95	71.86
MDS <sub>all</sub>	40.65	<b>81.12</b>
ReAct	34.83	73.64
GradNorm	<b>75.65</b>	55.49
EBO	42.35	73.08
$D_\alpha$	41.11	70.18
Dice	51.23	67.63
ViM	32.46	74.06
Ens-V (us)	46.19	74.91
Ens-R (us)	47.73	77.02
Ens-F (us)	41.75	78.03

Table 11: AUC for OOD detection in DSD setting for ResNet on corruptions datasets.

	defocus blur	Gaussian noise	snow	brightness
Accuracy %	15.04	5.68	15.58	55.64
CADet $m_{in}$	96.17	95.24	86.47	70.70
ODIN	97.17	99.01	89.22	68.66
Max logits	96.54	97.65	93.76	75.53
Logits norm	87.48	90.37	86.04	67.36
MSP	94.05	94.88	87.57	70.32
MDS <sub>f</sub>	46.35	98.34	88.67	72.70
MDS <sub>l</sub>	68.85	96.44	78.72	56.96
MDS <sub>all</sub>	92.87	99.52	91.28	73.99
ReAct	94.88	97.01	94.09	73.31
GradNorm	98.02	96.97	90.06	72.51
EBO	96.62	97.86	94.29	75.78
$D_\alpha$	94.66	95.66	88.61	70.80
Dice	97.81	98.08	93.47	<b>76.16</b>
ViM	83.9	97.11	94.19	72.80
Ens-V (us)	97.39	<b>99.68</b>	94.62	72.64
Ens-R (us)	97.04	99.57	93.58	72.04
Ens-F (us)	<b>98.13</b>	99.41	<b>94.96</b>	73.84

Table 12: AUC for OOD detection in DSD setting for ResNet on adversarial attacks dataset. PGD ResNet denotes PGD computed against ResNet (hence white box), and PGD ViT against a separate ViT model (hence black box).

	PGD ResNet	AA ResNet	PGD ViT	AA ViT
Accuracy %	2.2	25.8	68.12	43.2
CADet $m_{in}$	45.37	71.11	<b>64.86</b>	68.25
ODIN	12.91	79.70	54.98	70.18
Max logits	18.54	<b>84.50</b>	59.42	<b>76.01</b>
Logits norm	13.47	70.21	58.31	65.30
MSP	30.82	82.23	58.02	73.59
MDS <sub>f</sub>	71.17	55.59	44.73	48.67
MDS <sub>l</sub>	88.19	74.36	46.81	66.26
MDS <sub>all</sub>	86.00	81.05	46.83	72.07
ReAct	33.02	82.62	55.62	74.56
GradNorm	15.62	77.67	63.52	69.25
EBO	18.52	84.46	59.42	75.97
$D_\alpha$	30.62	82.90	58.13	74.11
Dice	16.55	82.78	61.34	74.35
vim	39.40	82.85	54.30	75.10
Ens-V (us)	<b>91.56</b>	81.12	54.91	71.81
Ens-R (us)	89.19	82.88	55.28	73.48
Ens-F (us)	66.86	83.38	54.13	72.89

Table 13: AUC in error detection setting for ResNet.

	In-Dist	Adv. Attacks				Corruptions			
		PGD RN	AA RN	PGD ViT	AA ViT	blur	noise	snow	bright.
CADet $m_{in}$	56.50	46.09	79.56	68.22	77.52	97.3	96.16	89.08	77.91
ODIN	75.79	15.23	90.02	60.53	86.05	99.05	99.68	94.42	86.91
Max logits	77.55	21.99	<b>94.58</b>	65.26	91.63	98.9	99.10	97.66	91.68
Logits norm	50.11	13.94	76.73	59.98	73.11	88.88	90.96	87.52	70.13
MSP	<b>86.31</b>	38.06	94.06	71.87	92.16	98.34	97.97	94.65	92.76
MDS <sub>f</sub>	51.25	71.44	54.82	45.66	54.72	46.12	98.44	88.89	72.44
MDS <sub>l</sub>	55.53	<b>88.45</b>	80.97	46.25	73.87	68.74	96.35	79.15	59.14
MDS <sub>all</sub>	54.69	85.67	85.00	47.96	79.96	93.14	99.54	91.67	75.23
ReAct	73.28	37.80	92.24	58.27	88.95	97.25	98.28	97.05	87.46
GradNorm	58.07	16.41	86.52	67.03	79.99	98.85	97.84	93.01	81.21
EBO	76.02	21.82	94.12	63.70	90.86	98.76	99.08	<b>97.68</b>	90.93
$D_\alpha$	86.20	37.90	94.42	71.05	<b>92.52</b>	98.56	98.3	95.16	<b>93.00</b>
Dice	70.00	19.15	91.50	65.13	87.05	98.94	98.84	96.19	88.13
ViM	73.74	43.99	92.62	54.47	88.23	89.90	98.52	97.13	86.58
Ens-V(us)	72.81	80.72	86.67	72.03	82.44	98.40	<b>99.80</b>	96.59	84.12
Ens-R (us)	77.24	78.62	90.66	78.41	87.48	99.26	99.68	97.20	87.52
Ens-F (us)	79.20	73.25	90.45	<b>79.09</b>	87.61	<b>99.28</b>	99.73	<b>97.68</b>	89.26

Table 14: AUC for OOD detection in DSD setting for ViT.

Acc %	iNat	OI-O	INet-O	PGD-R	AA-R	PGD-V	AA-V	Biggan	diff	blur	noise	snow	bright
-	-	-	-	77.00	65.22	0.46	50.66	86.28	55.77	42.09	42.85	56.82	76.12
CADet	8.30	24.83	29.61	63.06	77.29	60.64	67.48	68.72	50.92	98.12	72.45	78.37	69.72
ODIN	97.05	93.85	84.28	57.76	72.44	11.92	67.02	49.19	76.28	87.23	93.96	76.72	60.81
Max logits	98.65	97.06	90.04	63.68	76.44	24.82	73.96	54.87	77.28	94.24	90.97	83.20	66.00
logits norm	50.84	51.70	53.24	41.58	39.26	31.18	37.52	42.61	33.89	41.62	41.91	35.54	40.89
MSP	96.39	92.99	82.31	61.61	71.99	26.64	73.57	54.81	74.74	88.83	85.71	77.11	62.82
MDS <sub>f</sub>	66.73	53.68	39.63	68.59	77.31	68.76	56.24	49.04	60.79	40.95	62.54	07.00	15.39
MDS <sub>i</sub>	<b>99.63</b>	<b>98.22</b>	<b>94.28</b>	68.59	76.34	<b>78.54</b>	75.54	53.61	84.35	82.32	97.22	85.07	68.56
MDS <sub>all</sub>	90.37	89.88	87.25	80.06	<b>91.74</b>	78.49	<b>92.26</b>	54.09	<b>90.81</b>	99.74	99.99	<b>96.14</b>	<b>86.31</b>
ReAct	98.67	97.12	90.62	64.09	75.22	29.99	73.52	54.95	77.10	93.62	90.95	83.23	66.87
GradNorm	97.35	94.53	80.68	67.47	84.36	35.00	73.83	73.79	70.59	99.00	88.32	83.17	69.50
EBO	98.69	97.26	90.61	63.68	76.5	25.20	73.48	54.8	77.02	94.54	91.20	83.48	66.11
$D_\alpha$	97.03	93.76	83.02	61.74	72.30	26.67	73.77	54.81	75.08	89.41	96.29	77.58	62.99
Dice	51.43	63.67	51.99	<b>83.91</b>	89.67	62.91	76.68	<b>86.29</b>	69.39	96.56	80.85	87.12	82.13
ViM	98.88	97.07	91.33	61.36	69.30	26.72	70.00	46.87	75.15	82.01	91.90	81.50	63.75
Ens-V(us)	99.00	96.28	89.64	75.48	<b>92.23</b>	73.67	89.28	71.27	85.62	<b>99.89</b>	<b>99.99</b>	92.11	79.06
Ens-R (us)	98.90	96.59	89.50	71.47	90.74	72.37	88.58	68.38	84.74	99.86	<b>99.99</b>	91.40	77.41
Ens-F (us)	98.42	96.55	90.27	73.46	90.33	64.72	87.70	64.37	85.66	99.33	99.97	90.87	76.11

Table 15: AUC in error detection setting for ViT.

	In-Dist	Adv. Attacks				Corruptions			
		PGD-R	AA-R	PGD-V	AA-V	blur	noise	snow	brightness
CADet $m_{in}$	49.73	63.59	83.42	60.59	72.46	98.75	75.98	80.88	70.60
ODIN	75.02	60.76	85.12	13.26	68.76	95.20	98.41	89.54	80.18
Max logits	80.64	71.08	91.30	27.84	80.47	99.03	98.07	95.95	89.13
Logits norm	36.83	41.91	34.12	29.06	31.12	39.59	38.48	27.87	28.65
MSP	<b>89.16</b>	77.15	92.01	30.80	81.19	98.29	97.28	95.46	91.95
MDS <sub>f</sub>	48.23	67.86	81.36	68.65	54.84	40.29	61.60	06.84	14.08
MDS <sub>i</sub>	74.92	75.46	88.62	<b>82.28</b>	85.57	91.23	99.45	95.25	99.64
MDS <sub>all</sub>	54.93	83.08	95.24	81.01	<b>98.42</b>	99.80	99.99	96.92	<b>99.68</b>
ReAct	77.18	69.62	89.09	33.15	80.12	98.56	97.56	95.26	87.87
GradNorm	68.01	72.49	93.74	37.21	80.24	99.79	96.48	94.31	85.42
EBO	78.35	68.77	90.13	28.07	79.54	98.90	97.82	95.48	87.82
$D_\alpha$	89.00	76.97	92.31	30.82	81.37	98.49	97.54	95.74	92.05
Dice	50.09	85.18	93.85	63.02	80.35	97.61	85.60	89.82	83.47
ViM	75.72	65.66	82.18	29.50	76.14	90.59	97.81	93.58	84.59
Ens-V(us)	82.61	92.73	96.22	74.58	94.54	<b>99.99</b>	<b>100.00</b>	98.64	94.46
Ens-R (us)	83.69	90.15	95.39	73.09	94.06	<b>99.99</b>	<b>100.00</b>	98.15	93.23
Ens-F (us)	85.84	<b>93.42</b>	<b>96.54</b>	70.43	94.47	99.97	<b>100.00</b>	<b>98.78</b>	94.88